Available online at www.sciencedirect.com
ScienceDirect
International Journal of Heat and Mass Transfer 49 (2006) 5062–5069
International Journal of HEAT and MASS TRANSFER
www.elsevier.com/locate/ijhmt

Numerical study and optimization of the porous media VOC oxidizer with electric heating elements

N.N. Gnesdilov *, K.V. Dobrego, I.M. Kozlov, E.S. Shmelev

Heat and Mass Transfer Institute, National Academy of Sciences of Belarus, P. Brovki Street 15, Minsk 220072, Belarus

Received 24 February 2006
Available online 1 August 2006

Abstract

Porous media VOC oxidizing reactor, consisting of coaxial tubes system with counter-flow heat exchange and embedded electric heater, is under investigation. Influence of heater configuration and power, gas flow rate and thermal isolation on maximum temperature in reactor and unburned VOC concentration is determined numerically. It is shown that axial configuration of the heater is more effective than the circular one in the case of high flow rates $U_G \sim 1$ m/s or more. Minimum unburned VOC is reached if axial heater end is set at the level of the central tube edge.

Practical porous media VOC oxidizer was simulated for the aim of the mathematical model verification. Comparison of simulated and measured non-steady temperature fields in the reactor during startup demonstrate reasonably good agreement (10–20%).

Keywords: Porous media combustion; Heat recuperation; Heating element; Porous media; Volatile organic components (VOC)

1. Introduction

Recreation of polluted flue gases remains an actual problem for a variety of mechanical, chemical and biochemical technologies [1,2]. Flue gas purification may be performed by either capturing of admixtures or their chemical transformation to the neutral or valuable chemical species. There is a variety of industrial methods of flue gases purification: sorption, condensation, combustion (conventional or catalytic), membrane separation, chemical/biochemical transformation of pollutants to neutral or easily utilizable components [1,2]. All the mentioned methods are rather specific. The sorption process of gas purification consumes sorbents which have limited lifetime and demand its recreation or replacement. Condensation to liquid phase is appropriate only to components characterized by relatively high temperature of condensation and in the case of high concentration of pollutants [1]. Direct combustion of the polluted air in the open flames is not effective economically if the process is not combined with industrial boiler, furnace or power generator. Membrane separation, catalytic oxidizing, chemical or biochemical transformation of the pollutants all remain expensive technologies, rather selective and therefore may be efficient only for specific cases [1,2].

The widely spread air pollutants – volatile organic components (VOC) – methane, phenol, formaldehyde, acetone, benzol and others are contained in ventilation gases of mines, paint shops, plastic extruder shops, in technological flue gases, etc. In many cases VOCs concentration is less than combustion lean limit concentration, but enough for self-sustained combustion in inert porous media. Combustion in inert porous media (or filtration combustion) provides effective heat recirculation and consequently low energy costs of the process [3–6]. In the case of sufficiently high concentration of VOCs (~1 mass%) the combustion process may be sustained due to heat content of the pollutants and does not demand any additional fuels. In experiments by Takeno and Sato [7] in a steady reactor with complicated heat recuperation methane–air mixture

* Corresponding author. Tel.: +375 172842217; fax: +375 172842212.
E-mail address: nick_gn@itmo.by (N.N. Gnesdilov).

0017-9310/$ - see front matter © 2006 Elsevier Ltd. All rights reserved.
doi:10.1016/j.ijheatmasstransfer.2006.06.001

Nomenclature

c_p	gas specific heat, J/kg/K
c_s	porous media specific heat, J/kg/K
d_0	diameter of packed bed particle, m
d_1	central tube diameter, m
d_2	reactors (computation domain) diameter, m
$\mathbf{D}$	gas diffusivity tensor, include gas diffusivity and dispersion diffusivity
G	gas flow rate, m^3/h
h_i	mass enthalpy of ith gas component, J/kg
k_0,k_1	Ergun's constants in gas filtration equation
m	porosity
M	mean molar mass of gas mixture, kg/mol
p_0	pressure at exit of reactor, Pa
r	radius, m
R	universal gas constant, J/mol/K
t	time, s
T_0	initial temperature, K
T	temperature, K
T_{ad}	gas mixture adiabatic combustion temperature, K, $\Delta T_{ad} = T_{ad} - T_0$
$T_{g,max}$	maximum temperature of gas, K
$T_{s,max}$	maximum temperature porous media, K
$\Delta T_E = \frac{W}{G(c_p\rho_g)\vert_{T=T_0}}$	electric heater heating up temperature, K
$\mathbf{u}$	gas filtration velocity, m/s
$U_G = G/S$	superficial gas velocity, m/s
W	electric heater power, W
W_e	electric heater power per heater volume, W/m^3
X_i	mole concentration of ith gas component, mol/mol
X_{CH_4}	methane mole concentration at exit of reactor
Y_i	mass fraction of ith gas component, kg/kg
z	coordinate, m
z_0	coordinate of upper edge of electric heater, m
z_1	central tube length, m
z_2	reactor's (and computation domain) length, m

Greek symbols

α	heat transfer coefficient, $W/K/m^2$
α_{vol}	volumetric heat transfer coefficient, $W/K/m^3$
ε	surface emissivity of the packed bed particle
$\mathbf{\Lambda}$	heat conductivity of gas tensor, $\mathbf{\Lambda} = c_p\rho_g\mathbf{D}$
λ	effective heat conduction coefficient of packed bed, W/K/m
μ	gas viscosity, Pa s
ρ	density, kg/m^3
$\dot{\rho}_i$	ith component generation rate in chemical reaction, kg/s
Φ	fuel/oxidizer equivalence ratio

Indexes

1	relates to internal tube
2	relates to external tube
g	gas
s	solid
i	ith component of gas mixture

combustion was realized at equivalence ratio as low as $\Phi = 0.026$ (which is 20 times lower than lean limit combustion concentration for methane–air mixture). In the work [3,4] the regenerative porous media reactor was utilized for lean methane combustion. The stable combustion was achieved at equivalence ratio $\Phi = 0.15$.

Physical aspects of the FC in inert porous media are discussed in [4,7,8] and other papers. One of the principal features of FC is internal heat recirculation in the combustion wave, due to heat exchange between gas and solid in the preheat zone of the combustion wave. Practical systems designed for the low calorific fuels combustion utilize schemes of external heat recirculation in addition to the internal one. These are heat recuperation by means of counter-flow heat exchange between incoming and exhaust gases and heat regeneration due to periodical reverse of flow direction. Both schemes are investigated in laboratory installations [3,4,9–11] and found their application in industrial VOCs oxidizers, produced by Thermatrix [12], ReEco-Stroem [13] and other companies. In the work [14] the combined regenerator–recuperator scheme of the reactor is investigated numerically. It is shown that new scheme let one expand the range of operational flow rate and VOC concentration.

Utilization of electric heaters embedded into porous media of the oxidizer allows one to eliminate limitation on VOC concentration and guarantees control over the thermal regime of the burner. The embedded electric heaters are already in use in some reactors [12], nevertheless theoretical or experimental investigations on heaters design influence on rector's performance are not known to the authors.

In this article numerical study of the steady-state recuperative reactor with embedded electric heater is performed. The influence of geometrical configuration of the electrical heater and its position on temperature parameters and VOC burning out is under investigation. The numerical model verification is performed by comparison with experimental data obtained at UDG-2 VOC oxidizer, built in Heat and Mass Transfer Institute, Minsk [15].

The chemical kinetics of VOC oxidation is modeled by four-step brutto mechanism for acetone combustion in UDG-2 reactor and one-step brutto model for methane combustion in all other simulations.

It is shown that axial configuration of the electric heater is preferable at average and elevated flow rates. Minimal concentration of unburned hydrocarbons is provided when heater is placed at the level of top edge of the central tube.

2. Problem statement

The system under investigation consists of two coaxial tubes, filled with ceramic particles (Fig. 1). VOC containing gas enters through central tube passes by electric heater and goes out through external tube. Due to heat exchange with the porous media gas warms up and gets additional heat from embedded electric heater. At certain temperature VOC oxidation starts and combustion products heat up porous media and incoming fresh gas via it.

We considered two configurations of electric heater for parametric study. First, cylindrical heater (0.01 m diameter and 0.2 m length) is placed at the axis of the reactor with the z_0 coordinate of the upper end (Fig. 1 (6)). In other case heating element has ring type geometry (Fig. 1 (7)). It placed at the surface of central tube and has the following dimensions: height – 0.2 m; diameter – 0.1 m and width – 0.005 m. Heating elements are not permeable for gas.

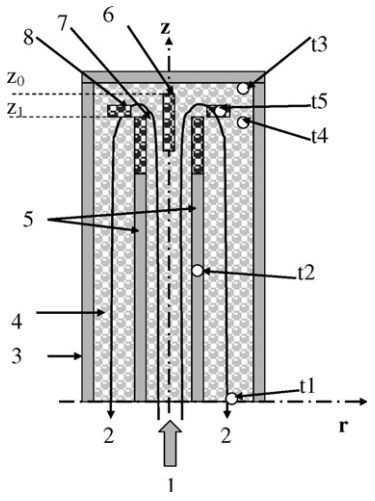

Fig. 1. Scheme of the reactor and heating elements configuration. (1) Incoming gases, (2) flue gases, (3) reactors body, (4) porous media, (5) central tube, (6)–(8) electric heater; (6) axial position, (7) ring shape element, (8) ring shape element for UDG-2 reactor simulation. t1–t5 are positions of thermocouples.

For numerical simulation of experimental UDG-2 reactor ring type configuration of the electric heater was taken (Fig. 1 (8)). The volume of the model heater corresponded to the experimental one. The height, the internal and the external radius of the ring are 0.5, 5.5 and 4.5 cm correspondingly. Thermocouple position in the experimental reactor are given in (z,r) coordinates: t1 – $(0,0.08)$, t2 – $(0.34,0.045)$, t3 – $(1.08,0.08)$, t4 – $(1,0.08)$, t5 – $(1.027,0.09)$.

3. Governing equations

Conventional volume averaged approximation was used for simulation of the system [14,16,17]. The set of equations included continuity and filtration equations for gas, mass conservation equation for chemical components, thermal conductivity equations for gas and solid phases, and ideal gas state equation. Gas dispersion conductivity and diffusivity is used in diffusion and conduction equations (3) and (4) [18]. Radiation conductivity is taken into consideration in the heat conductivity equation for porous media (5). One can find more detailed description of the mathematical model, boundary conditions and algorithms in [14,16,17].

$$\frac{\partial \rho_g}{\partial t} + \nabla(\rho_g \mathbf{u}) = 0. \tag{1}$$

$$-\nabla p = \frac{\mu}{k_0}\mathbf{u} + \frac{\rho_g}{k_1}|\mathbf{u}|\mathbf{u}. \tag{2}$$

$$\rho_g \frac{\partial Y_i}{\partial t} + \rho_g \mathbf{u}\nabla Y_i - \nabla \rho_g \mathbf{D}\nabla Y_i = \dot{\rho}_i. \tag{3}$$

$$\rho_g c_p \frac{\partial T_g}{\partial t} + c_p \rho_g \mathbf{u}\nabla T_g - \nabla \mathbf{\Lambda} \nabla T_g = \frac{\alpha_{vol}}{m}(T_s - T_g) - \sum_i h_i \dot{\rho}_i. \tag{4}$$

Table 1
Standard values of the problem parameters

Parameter	Dimension	First value	Second value	Parameter description
z_0	m	0.82	1.03	Coordinate of electric heater
z_1	m	0.82	1.0	Central tube length
z_2	m	1	1.23	Reactor length
d_0	m	1.5×10^{-3}	2.3×10^{-2}	Packed bed particle diameter
d_1	m	0.1	0.09	Central tube diameter
d_2	m	0.16	0.17	Reactor diameter
T_0	K	300	300	Initial temperature of the system
p_0	Pa	1.01325×10^5	1.01325×10^5	Pressure at exit of reactor
ε	–	0.35	0.3	Emissivity of the packed bed particles
m	–	0.5	0.64	Porosity
ρ_s	kg/m^3	1750	2248	Packed bed material density
c_s	J/kg/K	1300.0	1200	Packed bed material heat capacity
λ_s	W/m/K	0.2	0.2	Packed bed material thermal conductivity coefficient
λ_{sw}	W/m/K	0.2	1.0	Thermal conductivity of the reactor walls
D_p,D_τ	m^{-1}	0.5, 0.1	0.5, 0.1	Dispersion coefficients for diffusivity and conductivity
Φ	mol/mol	0.02	~0.066	Fuel oxidizer equivalence ratio
α	W/m^3/K	$\sim 10^5$	$\sim 7 \times 10^4$	Heat transfer coefficient
G	m^3/h	15	~3.0	Total gas flow rate
U_G	m/s	0.66	~0.13	Gas superficial velocity
ΔT_E	K	272.5		Temperature of electric heat up of the gas mixture

Table 2
Models of chemical kinetics of methane and acetone oxidation

Reaction	Reaction rate	Ref.
(1) $CH_4 + 2O_2 \xrightarrow{k} CO_2 + 2H_2O$	$k = 2.17 \times 10^8 \exp(-15{,}640/T)$	[19]
(2) $2C_3H_6O + 5O_2 \xrightarrow{k} 6CO + 6H_2O$	$k = 1.95 \times 10^{16}(pT)^{-1}\exp(-25{,}191/T)$	[19]
(3) $2H_2 + O_2 \xrightarrow{k} 2H_2O$	$k = 7.73 \times 10^9 p^{-2.5}\ T^{-0.5}\exp(-10{,}575/T)$	[19]
(4) $2CO + O_2 \xrightarrow{k} 2CO_2$	$k = 1.144 \times 10^{13}(pT)^{-1.5}\exp(-10{,}575/T)$	[19]
(5) $CO + H_2O \underset{kr}{\overset{k}{\leftrightarrows}} CO_2 + H_2$	$k = 1.22 \times 10^{13}(pT)^{-1}\exp(-20{,}897/T)$ $kr = 3.78 \times 10^{14}(pT)^{-1}\exp(-24{,}724/T)$	[19]

$$(1-m)\rho_s c_s \frac{\partial T_s}{\partial t} - \nabla(\lambda \nabla T_s) = \alpha_{vol}(T_g - T_s) + W_e. \quad (5)$$

$$\rho_g = \frac{pM}{RT_g}. \quad (6)$$

The systems (1)–(6) is added by boundary conditions for temperature, concentration and velocity. Adiabatic or Newtonian condition may be applied as boundary conditions for temperature. Tube walls impermeability is applied for gas component concentration and velocity. Fixed gas flow rate at entrance cross section of the system and constant pressure $p = p_0$ at exit conditions are used for filtration equation solution.

The values of parameters of the system in the standard case are presented in Table 1. All simulations are performed at the first value of the parameters (third column of Table 1) with the axial position of electric heater. Methane combustion is modeled by one-step reaction (1). Model verification and comparison with experimental UDG-2 burner were performed at the second value of the system parameters (column 4 of Table 1). The acetone combustion is simulated by four-step brutto reaction (2)–(5), Table 2.

2DBurner software package was used to solve two-dimensional problem (1)–(6) [17]. Non-steady solution was used for experimental data simulation and steady-state solution – for parametric study of the model system.

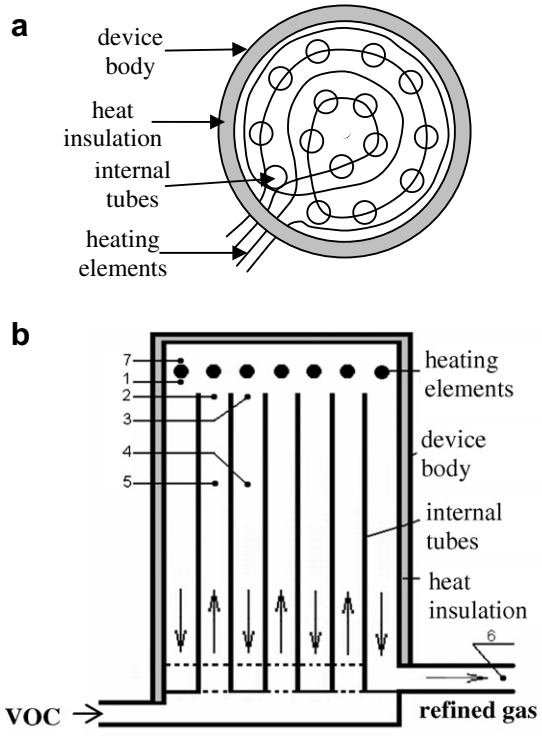

Fig. 2. Schematic of the VOC oxidation reactor UDG-2. (a) Upper sight with the lid removed, (b) schematic cross section. Figures – thermocouples position.

4. Model verification

Adequacy of the physical and mathematical models was tested by simulation of non-steady temperature field at the UDG-2 reactor startup and compared with results of numerical simulation.

VOC oxidation of the UDG-2 reactor is performed in the layer of alumina elements preheated by electric heater. Gas is fed to the hot zone by 15 tubes homogeneously distributed in the cross section of the reactor (Fig. 2). Hot combustion products are fed via inter-tube space counter flow to the incoming gas providing heat recuperation in the system. Electric heaters are three spirals of 2 mm nichrome wire, placed in ceramic beads with electric resistance of 6.9 Ohm each one. Spirals are powered from 3-phase network.

To control temperature at the heater a quartz shielded thermocouple is attached to the heater. Heating power control is realized by means of programmed switch on/off intervals. Typical gas flow rate in the reactor is 50 Nm^3/h and maximum electric heater power is 15 kW. Schematic representation of the reactor is given in Fig. 2. Thermocouple coordinates are given in the previous section. Reactor chamber diameter is 0.635 m, height, 1.235 m; central tubes diameter is 0.092 m and length, 1 m.

As far as 3D simulation of reactor as a whole is too complicated problem, an axis symmetrical element of the reactor (Fig. 1) was simulated. Diameter of the simulated system corresponded to the one-fifteenth part of the UDG-2 device cross section. Gas flow rate and electric power for simulated system were taken as one-fifteenth part of the practical device. Dimensions of the central tube and height of the simulation domain corresponded to the characteristics of the practical device. Acetone–air mixture was used as a combustible for simulations (model air composition was $N_2{:}O_2 = 79{:}21$). At a molar acetone to air ratio 0.66:100, $\Phi = 0.14$ and adiabatic combustion temperature of the mixture was $\Delta T_{ad} = 365.5$ K.

Fig. 3 represents measured (markers) and numerically estimated temperature in the points of thermocouples

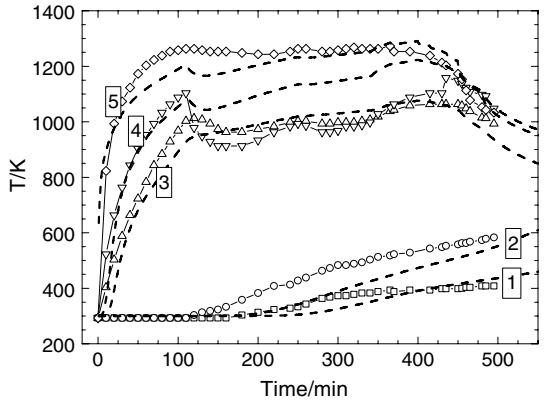

Fig. 3. Measured (markers) and simulated (lines) evolution of the temperature in the control points of reactor. Figures correspond to numbers of thermocouples.

Table 3
System parameters variation during startup of UDG-2 oxidizer

Time (min)	Electric power (W)	Gas flow rate (m^3/h)	Acetone concentration $X_{acetone}$ (%)
0–110	800	0.0	0
110–250	800	2.547	0
250–340	800	3.04	0
340–366	800	3.33	0.329
366–400	753	3.33	0.329
400–415	660	3.33	0.329
415–430	600	3.33	0.329
430–436	547	3.33	0.329
436–450	450	3.33	0.329
450–480	180	3.33	0.329
480–600	0.0	3.33	0.656

position during reactor's startup and transition to the steady-state operation regime. A typical reactor startup regime was simulated. Time table of the system parameters during startup (Table 3) was reproduced in simulation. Time interval in minutes is presented in the first column. Electric heater power, gas mixture flow rate and acetone concentration are presented in columns 2, 3 and 4 correspondingly. Parameters which were used for simulation are in Table 1. Note that corresponding power and flow rate for practical device is 15 times higher.

It is seen that evaluated temperature and temperature growth rates correspond well to the measured values. Observed mismatch can be explained by minor differences from tube to tube in the device, natural non-homogeneity of the packed bed, inaccuracy in determination of position of thermocouples and model inaccuracy. Nevertheless simulation results evidence good accuracy and adequacy of mathematical model of the system.

5. Parametric study results and discussion

Main parameters important for design and proper exploitation of the oxidizer are maximum temperature of the gas ($T_{g,max}$), solid ($T_{s,max}$) and unburned VOCs concentration at the exit of reactor – X_{CH_4}. Lean methane–air mixture was used as combustible in all parametric study simulations (equivalence ratio $\Phi = 0.02$, methane concentration $X_{CH_4O} = 0.001996$, air composition $N_2{:}O_2 = 80{:}20$). Mixture enthalpy is $\Delta H = 5.7 \times 10^5$ J/kg, adiabatic combustion temperature $\Delta T_{ad} = 530$ K, density and capacity at standard conditions: $\rho_g = 1.16$ kg/m^3, $c_p = 1025$ J/kg/K.

We investigate influence of the heater position and configuration, electric heater power, mixture flow rate on the abovementioned parameters. Let us characterize electric heating power by two parameters: electric power W and temperature gain due to electric heating ΔT_E, according to formula

$$\Delta T_E = \frac{W}{G(c_p\rho_g)|_{T=T_0}}. \quad (7)$$

5.1. Fixed heat up temperature ΔT_E

Mixture flow rate increase at other fixed parameters of the system results in combustion of front downstream shift and decrease of both gas and solid maximum temperature. Then electric heat up temperature $\Delta T_E = 272.5$ K is fixed (due to variation of electric power) temperature dependence on gas flow rate changes. Fig. 4 demonstrates slow decrease of $T_{g,max}$ (curves 4–6) and increase of $T_{s,max}$ (curves 7–9) with flow rate growth. This peculiarity is explained by linear growth of heating power W with U_G and slower than linear growth of heat transfer from solid to gas [14,18], resulting in minor growth of the solid body temperature.

Variation of reactor design parameters such as central tube length and heater configuration may have strong effect on operation regime. The dependence of the unburned methane concentration X_{CH_4} at exit and maximum temperature of gas on gas flow rate is presented in Fig. 4 for the central tube lengths: 0.82 (squares) and 0.9 m (circles). It

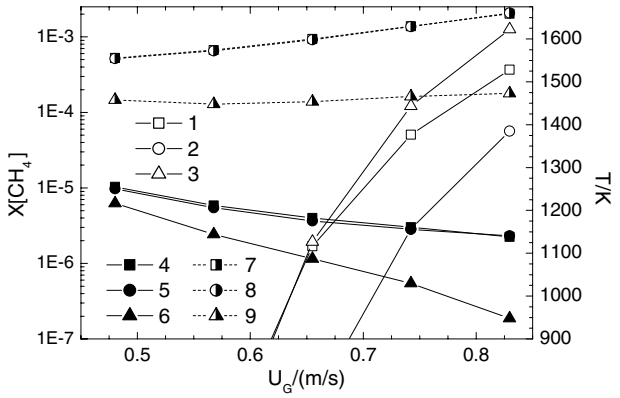

Fig. 4. Unburned methane concentration at exit X_{CH_4} (curves 1–3), gas maximum temperature $T_{g,max}$ (curves 4–6) and solid body temperature $T_{s,max}$ (curves 7–9) dependence on gas filtration rate. Squares stand for axial configuration of electric heater and internal tube length $z_1 = 0.82$. Circle stands for $z_1 = 0.9$ m and triangle designates circular configuration of heater. $\Delta T_E = 272.5$ K.

is inferred from the figure that maximum gas temperature $T_{g,max}$ is almost insensible to increase of the central tube length. At the same time central tube elongation leads to considerable decrease of unburned methane.

The same dependences, obtained for different (axis and circular) configurations of electric heaters are presented in Fig. 4. One can see that axial configuration of heater provides considerable overheating of gas compared to circular one. Meanwhile unburned methane concentration decreases slowly and only at relatively high gas flow rates $U_G > 0.66$ m/s. These results demonstrate that higher local $T_{g,max}$ do not guarantee complete burn out because of inhomogeneous temperature field in combustion area.

Thus axial configuration of electric heater better suits for higher mixture flow rates as far as low unburned VOC at exit (not higher temperature) is the principal requirement for this technology.

5.2. Fixed electric heating power

Regime with fixed electric heating power is technically simpler than constant ΔT_E regime. The main parametric dependences in this case are little different from the dependences at constant ΔT_E (specific power input) (Fig. 4). Calculated dependences of X_{CH_4} and $T_{g,max}$ on gas flow rate for two different powers of heaters – $W = 1200$ (designated by squares) and 1500 W (designated by circles) are presented in Fig. 5. One could see that at the same ΔT_E, unburned methane concentration is lower in the case of lower power input ($W = 1200$ W), in spite of the fact that gas maximum temperature is also lower in this case. This result is a sequence of the fact that lower W corresponds to lower U_G and more resident time for oxidation available.

5.3. Heating up at constant gas flow rate

Constant gas flow rate is one of the typical operation regimes of VOC burners. Several parametric dependences were built at $U_G = 0.66$ m/s. Unburned methane concentration at exit and temperatures $T_{g,max}$ and $T_{s,max}$ as a function of heat up temperature ΔT_E for different electric heater configurations are presented in Fig. 6. Square stands for axis and circle stands for circular heater configuration.

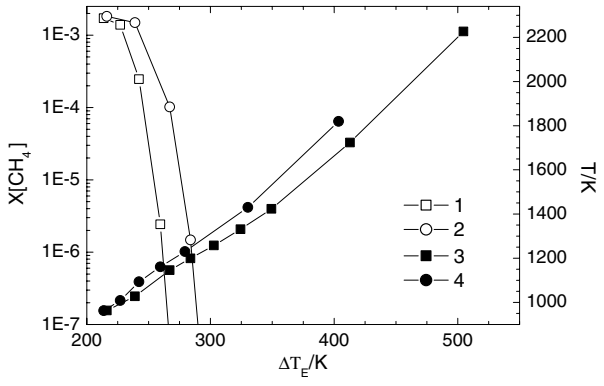

Fig. 5. Unburned methane concentration at exit X_{CH_4} – (1) and (2) and gas maximum temperature $T_{g,max}$ – (3) and (4) dependence on heating up temperature ΔT_E. $W = 1200$ W (curves 1 and 3) and 1500 W (curves 2 and 4).

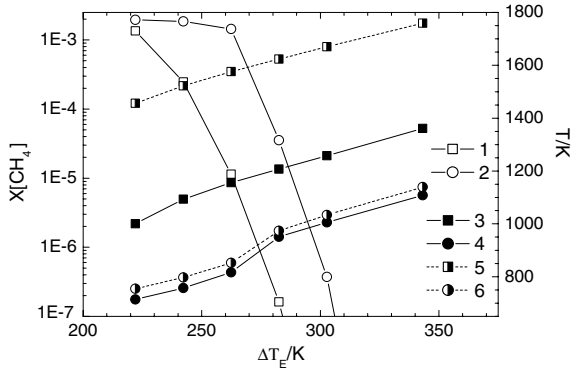

Fig. 6. Unburned methane concentration at exit X_{CH_4} (curves 1 and 2), maximum gas temperature $T_{g,max}$ (curves 3 and 5) and carcass $T_{s,max}$ (curves 4 and 6) dependence on ΔT_E for axis (curves 1, 3 and 5) and circular (curves 2, 4 and 6) configuration of the electric heater. $U_G = 0.66$ m/s.

One can see that maximal temperatures for circular heater (curves 4 and 6) is lower than at another case. It is explained by fact that in this case surface area of the heater is higher. Curves 4 and 6 in Fig. 6 demonstrate that VOC burning out starts from temperatures of heating $\Delta T_E \sim 260$ K. This fact explains rapid growth of temperatures in the region ΔT_E 260–280 K (twist of the curves 4 and 6). Comparing the same parameters for axis and circular heater configuration (Fig. 6) one can see that axial heater provides the same burnout efficiency at lower heat up temperature ΔT_E. Thus, in the case of fixed electric heat up (as well as in the case of constant power W) axis configuration of the heater is more effective.

5.4. Electric heaters efficiency at different thermal isolation conditions

Depending on thermal isolation conditions (design of insulation lining) efficiency of electric heaters can vary. Let us choose two types of insulation designs: (1) adiabatic reactor and (2) adiabatic reactor with unshielded upper butt-end. Suppose that heat exchange of unshielded butt-end with ambient air ($T_0 = 300$ K) is Newtonian with heat exchange coefficient $\alpha = 6.5$ W/m^2/K. Both types of reactors were simulated comparatively with axial electric heater. Position of the heater was varied. Simulation results are presented in Fig. 7.

It is inferred from the data presented in Fig. 7, that unburned methane concentration curve has minimum at $z_0 \approx 0.8$ m, which corresponds to better efficiency of VOC oxidation. Graphs presented in Fig. 7 demonstrate difference in operation regime of reactors with different isolation design. As one could expect, the absence of isolation on the butt-end results in a decrease of temperature in the reactor and growth of quantity of unburned methane at exit. Figure shows that the absence of isolation gives stronger

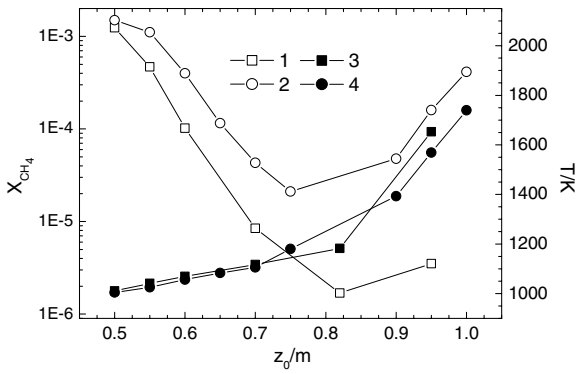

Fig. 7. Unburned methane concentration at exit X_{CH_4} (curves 1 and 2), maximum gas temperature $T_{g,max}$ (curves 3 and 4) dependence on heater coordinate z_0. Adiabatic reactor (curves 1 and 3) and reactor with unshielded butt-end (curves 2 and 4).

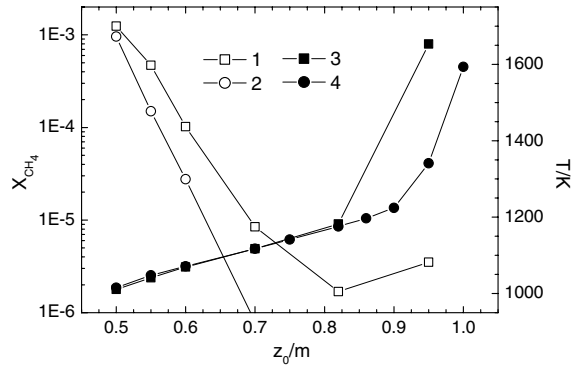

Fig. 8. Unburned methane concentration at exit X_{CH_4} (curves 1 and 2) and maximum gas temperature $T_{g,max}$ (curves 3 and 4), dependence on heater coordinate z_0. Central tube length $z_1 = 0.82$ m (curves 1 and 3) and $z_1 = 0.9$ m (curves 2 and 4).

effect on X_{CH_4} if the heater is closer to the upper butt-end (higher z_0 value). At the same time optimum position coordinate of the heater does not depend on thermal isolation conditions and remains $z_0 \approx 0.8$ m.

In spite of the expected heat loss growth from the butt-end with z_0 increase, maximum temperature in the system grows (Fig. 8). This fact is connected with rapid decrease of filtration flow near the upper end of the heater at $z_0 > z_1$. As a sequence, local temperature of porous body and gas grows, which nevertheless does not affect methane burnout. On the contrary, when heater comes out of the central tube $z_0 > z_1$, one can observe growth of X_{CH_4} due to underheating of the main stream of gas (Figs. 7 and 8).

Fig. 8 illustrates the influence of heater position on X_{CH_4} and $T_{g,max}$ for different central tube length. One can see that $T_{g,max}$ value is almost insensible to the tube length until the heater is placed inside the central tube. If the heater comes out of the central tube burn out turns for the worse. It is obviously connected with inefficient heat transfer to gas from the top part of the heater (placed out of central tube).

6. Conclusions

Porous media VOC oxidizing reactor, consisting of coaxial tubes system with counter-flow heat exchange and embedded electric heater is investigated numerically in the paper. Embedding of electric heaters is used to ensure combustion of very low heat content mixtures or in the case of strong variation of gas heat content or flow rate.

Numerical simulation of non-steady regime of the UDG-2 VOC oxidizer startup demonstrated good adequacy of the standard volume-averaged model of gas filtration combustion. A typical inaccuracy (10–20% in temperature) is of the order of natural differences in parameters from one tube to another in the device, non-homogeneity of packed bed, inaccuracy in determination of thermocouples position.

Based on parametric study of the model oxidizer the following conclusions may be done.

The longer central tube (as limited by pressure gap prerequisites, dimensions and thermal isolation oxidizer design) provides better heat recirculation, complete combustion and decreases energy consumption for electric preheat.

Axis configuration of the heater increases maximum gas and solid temperature in the system compared to circular configuration of the electric heater. However, the unburned methane concentration is the same for the axis and circular heaters configuration for the low ($U_G < 0.6$ m/s) gas flow rate. For the higher flow rates this parameter is better for axial burner configuration. At the same time axial configuration of heater gives higher non-homogeneity of temperature in hot zone which is a negative factor if thermotension or temperature resistance of the porous media is of critical importance.

Performed simulation let one optimize operation parameters of VOC oxidizer. In the case of simulated model reactor (methane concentration corresponds to $\Phi = 0.02$, other parameters as specified in Table 1), optimal heat up temperature $\Delta T_E \sim 275$ K. This value of ΔT_E provides low unburned methane concentration at exit $\sim 10^{-6}$ at reasonably low energy consumption.

Optimum position of the axial electric heater, providing minimum unburned methane concentration (Figs. 7 and 8) is secured when heater upper end position corresponds to the edge of central tube.

Analyzing quantitative results of the above study one should remember that all results are obtained for given model reactor and fixed set of thermodynamic and transport parameters of the system (Table 1). For optimization of VOC oxidizer in wide range of combustible concentration, specific geometry or structure of porous media additional simulations should be performed.

Acknowledgement

This work was supported by Belarusian Republican Foundation for Fundamental Research, Project T05-259.

References

[1] Selecting the most appropriate HAP emission control technology, Air Pollut. Consultant 3 (2) (1993) 1.1–1.9.

[2] Yu.S. Matros, A.S. Noskov, V.A. Chumachenko, Catalytic Recreation of Industrial Flue Gases, Nayka Publ., Novosibirsk, 1991, pp. 22–37 (in Russian).

[3] F. Contarin, A.V. Saveliev, A.A. Fridman, L.A. Kennedy, Int. J. Heat Mass Transfer 46 (2003) 949–961.

[4] L.A. Kennedy, A.A. Fridman, A.V. Saveliev, Superadiabatic combustion in porous media: wave propagation instabilities new type of chemical reactor, Int. J. Fluid Mech. Res. 22 (1995) 1–26.

[5] J.G. Hoffman, R. Echigo, H. Yoshida, S. Tada, Experimental study on combustion in a porous media with a reciprocating flow system, Combust. Flame 111 (1997) 32–46.

[6] W.D. Binder, R.J. Martin, The Destruction of Air Toxic Emissions by Flameless Thermal Oxidation, Presented at 1993 Incineration Conference, Knoxville, Tennessee, May 1993.

[7] T. Takeno, K. Sato, An analytical study on excess enthalpy flames, Combust. Sci. Technol. 20 (1979) 73.

[8] K.V. Dobrego, S.I. Zhdanok, Physics of filtration combustion of gases, HMTI Publishers, Minsk, 2002 (in Russian).

[9] K. Hanamura, R. Echigo, S. Zhdanok, Superadiabatic combustion in a porous medium, Int. J. Heat Mass Transfer 36 (13) (1993) 3201–3209.

[10] M.K. Drayton, A.V. Saveliev, L.A. Kennedy, A.A. Fridman, Y.E. Li, Superadiabatic partial oxidation of methane in reciprocal and counterflow porous burners, in: Proceedings of the 27th Symposium (International) on Combust, Pittsburg, PA, 1998, pp. 1361–1367.

[11] A.N. Migoun, A.P. Chernukho, S.A. Zhdanok, Numerical modeling of reverse-flow catalytic reactor for methane partial oxidation, Proceedings of the non-equilibrium processes and their applications. V International School-seminar, Minsk, 2000, pp. 131–135.

[12] www.thermatrix.com.

[13] www.eco-web.com.

[14] K.V. Dobrego, N.N. Gnesdilov, I.M. Kozlov, V.I. Bubnovich, H.A. Gonzalez, Numerical investigation of the new regenerator–recuperator scheme of VOC oxidizer, Int. J. Heat Mass Transfer 48 (2005) 4695–4703.

[15] To elaborate and to produce device for reburning of gaseous admixtures in exhaust gas fluxes of harmful plants, Final report. Treat 104, National Academy of Sciences of Belarus. A.V. Luikov Heat and Mass Transfer Institute, Minsk, 2003.

[16] K.V. Dobrego, I.M. Kozlov, S.A. Zhdanok, N.N. Gnesdilov, Modeling of diffusion filtration combustion radiative burner, Int. J. Heat Mass Transfer 44 (2001) 3265–3272.

[17] K.V. Dobrego, I.M. Kozlov, N.N. Gnesdilov, V.V. Vasiliev, 2DBurner – software package for gas filtration combustion systems simulation and gas non-steady flames simulation, Heat and Mass Transfer Institute, Minsk, 2004, Preprint N1.

[18] N. Wakao, S. Kaguie, Heat and Mass Transfer in Packed Beds, Gordon and Breach Science Publ., 1982.

[19] V.Ya. Basevich, A.A. Belyaev, S.M. Frolov, Global kinetic mechanism for turbulent reacting flow modeling. Part 1. Main chemical process of heat release, Chem. Phys. M. Nauka 17 (9) (1998) 117–129 (in Russian).